Basic Science

JOURNAL OF CHILDREN'S ORTHOPAEDICS

Growth modulation of angular deformities with a novel constant force implant concept-preclinical results

Jan Buschbaum[1]
Linda Freitag[1]
Theodor F. Slongo[2]
Stephan Zeiter[1]
Michael Schütz[3]
Markus Windolf[1]

Abstract

Purpose: Varus-valgus deformities in children and adolescents are often corrected by temporary hemi-epiphysiodesis, in which the physis is bridged by an implant to inhibit growth. With standard implant solutions, the acting forces cannot be regulated, rendering the correction difficult to control. Furthermore, the implant load steadily increases with ongoing growth potentially leading to implant-related failures. A novel implant concept was developed applying a controlled constant force to the physis, which carries the potential to avoid these complications. The study aim was to proof the concept *in vivo* by analyzing the effect of three distinct force levels on the creation of varus deformities.

Methods: The proposed implant is made of a conventional cerclage wire and features a twisted coil that unwinds with growth resulting in an implant-specific constant force level. The proximal medial tibial physes of 18 lambs were treated with the implant and assigned to three groups distinct by the force level of the implant (200 N, 120 N, 60 N).

Results: The treatment appeared safe without implant-related failures. Deformity creation was statistically different between the groups and yielded on average 10.6° (200 N), 4.8° (120 N) and 0.4° (60 N) over the treatment period. Modulation rates were 0.51°/mm (200 N), 0.23°/mm (120 N) and 0.05°/mm (60 N) and were constant throughout the treatment.

Conclusion: By means of the constant force concept, controlled growth modulation appeared feasible in this preclinical experiment. However, clinical trials are necessary to confirm whether the results are translatable to the human pathological situation.

Cite this article: Buschbaum J, Freitag L, Slongo T F, Zeiter S, Schütz M, Windolf M. Growth modulation of angular deformities with a novel constant force implant concept-preclinical results. *J Child Orthop* 2021;15:137-148. DOI: 10.1302/1863-2548.15.200218

Keywords: Temporary hemi-epiphysiodesis; varus-valgus deformity correction; growth modulation; growth inhibition by constant force

Introduction

Varus-valgus deformities (VVD) of the lower extremities are frequently encountered problems in children and adolescents.[1] Depending on the severity, surgical intervention is required otherwise VVD can lead to gait disturbance, knee instability and pain as well as pre-arthritic degenerative joint changes.[2] Provided there is sufficient growth of the patient remaining, VVD is often corrected by temporary hemi-epiphysiodesis. An implant is utilized to mechanically bridge the physis and locally restrict the growth of the growth plate. Through unrestricted growth on the opposite side the angular deformity is equalized.[3] The most common techniques for temporary hemi-epiphysiodesis are physeal stapling using Blount staples[4] or tension band plating (TBP), where the Eight-Plate (Orthofix Inc., Lewisville, Texas) is widely used.[5] The implant consists of a titanium plate and two titanium non-locking screws allowing angulation and thereby providing more flexible behaviour during treatment.[3,5,6] Superior outcomes with TBP over stapling were reported by various groups, as implant-related failures are less likely to occur.[7]

However, with existing implant solutions the loads applied to the physis and the forces acting on the implant during implantation are uncontrollable. Bylski-Austrow et al[8] showed in a biomechanical experiment on staples that the ongoing growth leads to a steady and non-linear rise of the reaction force of the fixation resulting in increased implant deformation. Devastating events like implant breakage or extrusion are frequently observed consequences.[2,3] Use of multiple staples increases the overall

[1] AO Research Institute Davos, Davos, Switzerland
[2] University Children's Hospital, Bern, Switzerland
[3] Queensland University of Technology Brisbane, Australia

Correspondence should be sent to Jan Buschbaum, Biomedical Development, AO Research Institute Davos, Clavadelerstrasse 8, 7270 Davos Platz, Switzerland.
E-mail: jan.buschbaum@aofoundation.org

stiffness resulting in higher forces acting on the physis which may result in permanent physeal closure.[9] These risks are mainly prominent with physeal stapling. However, once the screws of the TBP fixation reach maximum divergence they behave similarly to the staples.[10,11]

The load acting on the physis affects the amount of inhibited growth and thereby the correction rate, according to the 'Hueter-Volkmann Law'.[12] However, the forces exerted by the fixation and applied to the growth plate during treatment are not well understood, resulting in controversies about the working mechanism and effectiveness of the method. Stevens[6] reported approximately 30% faster correction using TBP compared with staples, explained by the theory of an extraphyseal fulcrum. Subsequent studies did not reveal significantly different correction rates between TBP and stapling.[13-16] Although the final correction was similar, Sanpera et al[11] and Goyeneche et al[17] found slower rates of early correction for TBP compared with staples, which is explained by the immediate exertion of compression with staples, whereas TBP is likely become effective only after a while.

In pre-clinical experiments Bonnel et al[18] and Stokes et al[19,20] applied constant compression forces to the physis and revealed different rates of inhibited growth in correlation with the force level. Bonnel et al[18] further observed a linear relationship between the amount of inhibited growth and time, indicating constant correction rates over the treatment period. Although growth regulation was proven feasible in animal experiments, the constant force principle has not yet been translated into a clinically usable implant and has never been tested in hemi-epiphysiodesis configuration. Inspired by these findings we hypothesize that applying a controlled and constant load to the physis can avoid aforementioned complications by enabling safe and reliable growth modulation. Therefore, we have developed a simple implant concept that integrates and applies a growth independent constant compression force to the physis. The aim of this study was to prove the concept in a large animal experiment by analyzing the effect of three different forces levels on creation of VVD.

Materials and methods

Novel constant compression implant

A new implant concept for applying a constant compression force to the growth plate was developed (Fig. 1). The implant is made of a conventional surgical cerclage wire (annealed stainless-steel) with two eyelets to attach the implant to the bone by standard non-locking screws bridging the physis. While one eyelet is a fixed loop, the other eyelet resembles a twisted coil with an open end. The functional principle of the implant can be understood as an extendible tension band. Under tension exerted by the epiphyseal growth, the coil unwinds from the screw, exhibiting a constant force to the physis that acts as resistance against the growth. Force generation is based on the principle of plastic deformation work on ductile metal required for unwinding the coil. The force level is determined by wire thickness and coil diameter. A video demonstrating the working principle can be found in the Supplementary Material. An illustration of the functionality is given in Figure 1. By means of a material testing machine (Instron 5866; Instron, Norwood, Massachusetts) equipped with a 1 kN load cell a prototype implant was extended at a constant displacement rate simulating bone growth. The implant elongates by unwinding the coil (Fig. 1b to 1d) resulting in a characteristic constant force acting against the direction of growth (Fig. 1a). This force is exerted to the physis until a predefined breaking point is reached and the function of the implant vanishes (Fig. 1d). The extension range can be customized by the number of coil windings and position of the laser cut breaking point. The implant does not require preloading before implantation.

In vivo study

In total, 18 Swiss White Alpine sheep were included in the study. The left medial tibial physis of each sheep was treated with the proposed implant in a hemi-epiphysiodesis setting (Fig. 2) aiming at creating a varus deformity.

Study design

The experiment was composed of an active phase for creation and examination of the varus deformity and a subsequent passive phase for observation of a potential rebound effect after the implant function has vanished. Termination of the active phase was event-driven, triggered either by a) detachment of the implant wire; or b) an achieved deformity of approximately 15°; or c) at least 5° deformity after six months. The resulting duration of the active phase was between four and six months. All animals with a deformity of > 5° after completion of the active phase underwent an additional surgery for implant removal and were included in the rebound investigation for up to three additional months. The surgeries were successively performed in three batches: pilot (n = 2, 200 N) and two main batches with n = 6 (n = 3, 120 N; n = 3, 60 N) and n = 10 (n = 2, 60 N; n = 3 120 N; n = 5, 200 N) animals.

Study groups

The animals were randomly assigned to three groups distinguished by the force level of the implant, exerting high (200 N, n = 7), medium (120 N, n = 6) or low (60 N, n = 5) forces.

JOURNAL OF CHILDREN'S ORTHOPAEDICS

Implants

Prior to surgery three implant types with 60 N, 120 N and 200 N constant force levels were produced in a standardized manner by bending surgical cerclage wires (thickness Ø1 mm, Ø1.25 mm and Ø1.5 mm; article numbers 291.130, 291.060, 291.050; DePuy Synthes Inc, Zuchwil, Switzerland) with a custom-made bending jig. The implant length was set to 16 mm (screw distance) and the extension range was limited to 6 mm by means of a laser cut notch acting as the intended breaking point. The eyelets were configured for use with Ø2.7 mm cortex screws (stainless steel, full thread, self-tapping; VS211.014-VS211.030, DePuy Synthes). The rigid loop was closed by means of laser welding.

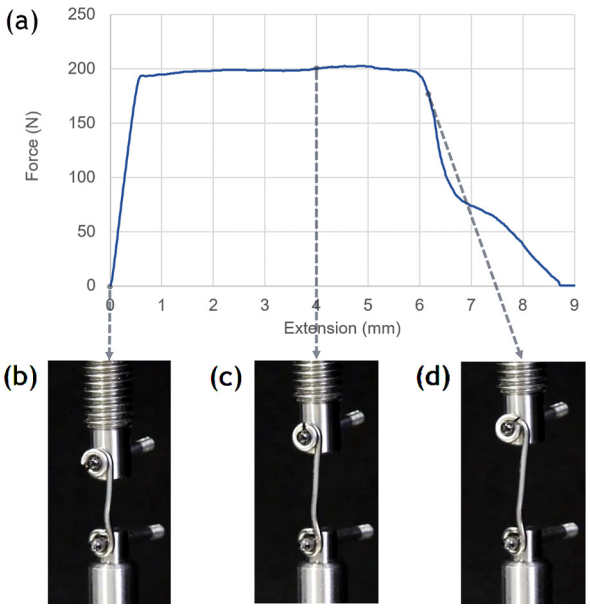

Fig. 1 Illustration of the implant functionality by means of a tensile test: a) resulting force-displacement curve; b) implant in initial position; c) during unwinding; and d) reaching predefined breaking point.

Animals and animal housing

Healthy (based on clinical examination and blood analysis), neutered male Swiss White Alpine sheep (mean age: 6.4 months (6 to 9); mean weight: 36 kg (23 to 48); Table 1) were obtained from a farmer and housed within the facility one month prior to the study start. Animals were group-housed throughout the study with a 12-hour light/dark cycle and received hey, straw, concentrated feed and water ad libitum.

Surgical protocol

After sedation with detomidine (Equisedan; Graeub AG, Bern, Switzerland; 0.04 mg/kg intramuscular) and intubation using midazolam Sintetica (Sintetica SA Mendrisio, Switzerland; 0.2 mg/kg intravenous) and ketamine (Ketasol-100; Graeub AG, Bern, Switzerland 4 mg/kg intravenous), general anaesthesia was maintained using sevoflurane (Baxter AG, Opfikon, Switzerland; 2 Vol% to 3 Vol%, 400 ml/min oxygen 200 ml/min air). For systemic analgesia the sheep received carprofen preemptively (Rimadyl Rind; Zoetis Schweiz GmbH, Delémont, Switzerland ; 1.4 mg/kg intravenous). All sheep received one dose of Ceftiofur (Excenel; Zoetis Schweiz GmbH, Delémont, Switzerland; 2.2 mg/kg intravenous) before the start of the surgery and every 90 minutes during surgery as antibiotic prophylaxis. The sheep were placed in left lateral recumbency and the left tibia was aseptically prepared. A skin incision on the medial aspect of the left proximal tibia was followed by blunt subcutane-

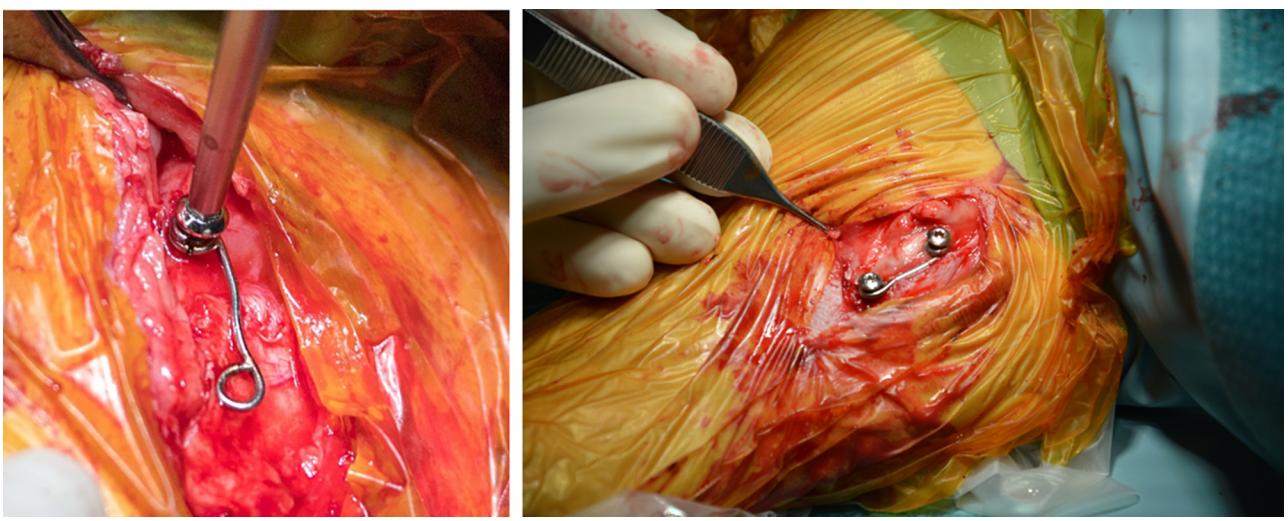

Fig. 2 Animal surgery during placement of the proposed implant.

Table 1 List with detailed information about the included animals

Animal	Implant group	Age at surgery, mths	Weight at surgery, kg	Active phase duration, wks	Passive phase duration, wks
1	200 N	7.1	23	16	12
2	200 N	7.1	24.5	12	-
3	200 N	6.0	35	26	10
4	200 N	6.3	39.5	26	10
5	200 N	5.7	32	26	10
6	200 N	5.5	30	26	10
7	200 N	6.1	39.5	26	-
8	120 N	7.1	41.5	36	-
9	120 N	7.0	36	36	-
10	120 N	6.6	32	36	-
11	120 N	6.0	33	36	-
12	120 N	5.7	37.5	26	10
13	120 N	6.3	48	26	10
14	60 N	6.5	34	26	-
15	60 N	8.7	47	26	-
16	60 N	6.4	48	14	-
17	60 N	6.0	35	26	-
18	60 N	5.9	35	26	-

ous preparation to expose the medial aspect of the bone. Under fluoroscopic control, the C-arm was aligned until perfect projection of the physis was achieved. A 1-mm Kirschner-wire was placed into the epiphysis in the medio-lateral direction, parallel to the axis of joint and physis. Insertion depth was approximately one-half to two-thirds of the epiphyseal width. Using a cannulated 2.0-mm drill, the pin hole was widened. The dynamic loop of the implant received a full threaded, Ø2.7-mm stainless steel cortex screw (VS211.014-VS211.030; DePuy Synthes) and was inserted into the epiphyseal hole. For drilling the metaphyseal hole, the rigid eyelet was used as a guide. A 1-mm pin was placed into the metaphysis in a parallel or slightly converging position to the proximal screw. Cooling and lavage during drilling were performed with a sterile ringer solution. Screw lengths were determined individually from preoperatively measured epi- and diaphyseal width (radiographs) and were intraoperatively confirmed via fluoroscopic control. The screw lengths were chosen to be between one-half and two-thirds of the epi- and diaphyseal width. The distal screw was fully tightened whereas the proximal screw was only tightened until the screw head touched the coil.

For growth tracking ten animals received radiopaque markers (1.5-mm cortex screw, stainless steel, self-tapping, length 10 mm; VS105.010, DePuy Synthes) in the epi- and metaphysis of the right tibia. The first eight animals had received stainless steel beads for tracking, which was found to be suboptimal due to observed loosening of the beads.

The surgical incision was closed in three layers (fascia, subcutis, skin) with absorbable (#3-0 non-cutting and cutting Monocryl, Ethicon, Johnson & Johnson AG, Zug, Switzerland) suture material in a continuous pattern. A spray dressing and a stent were placed for protection of the surgical site. All animals started weight-bearing right after surgery.

Removal surgery was carried out following the same surgical setting. Animals' burden was assessed using an institutional score sheet with predefined threshold for exclusion. At the study end all animals were euthanized with an overdose of intravenously administered pentobarbital (Esconarkon, Streuli Pharma AG, Uznach, Switzerland).

Data acquisition

Posteroanterior (PA) radiographs of the right and left tibias were taken postoperatively and then continued biweekly by use of conventional digital radiograph (Bucky Diagnost Trauma II; Philips Healthcare, Eindhoven, The Netherlands). CT scans were performed postoperatively and then monthly under general anaesthesia using clinical CT (SOMATOM Emotion 6; Siemens Healthcare GmbH, Erlangen, Germany; slice thickness 0.6 mm).

Evaluation of created deformity

The created varus deformity was evaluated by the change of the articular line-diaphysis angle (ALDA) on radiographs (Fig. 3b) as described in literature.[9,11,21] Measurements were performed using Synedra software (Synedra View Personal 17; Synedra Information Technologies GmbH, Innsbruck, Austria). The change of ALDA (ΔALDA) was calculated with respect to the postoperative measurement. For evaluation ΔALDA over time and with respect to growth was used. The modulation rate was determined as the ratio of ΔALDA per growth and assessed as a group mean over time. In an additional analysis, the relationship between the achieved modulation rate and applied normalized load was examined. The averaged modulation rate of each animal was related to the normalized load,

JOURNAL OF CHILDREN'S ORTHOPAEDICS

defined as the ratio of implant force divided by the animal's body weight.

Tibial growth measurement

Tibial growth was obtained from PA radiographs of the untreated right leg and measured by the increased distance between intersections of the diaphyseal axis with the proximal and distal articular lines (Fig. 3a). The prevailing growth at the proximal physis was analyzed by CT scans of the two radiopaque tracking screws in the untreated right leg. The generated Digital Imaging and Communications in Medicine data were imported into a custom-made MATLAB script (MATLAB 2017b; The MathWorks Inc, Natick, Massachusetts). This generated 3D isosurface models of the screws. The increase of the distance between centroids of the screws the proximal tibia growth was determined.

Implant elongation

The implant lengthening as a result of the unwinding of the coil was analyzed from CT scans by measuring the screw-to-screw distance (Fig. 3c). The 3D isosurface models of the implant generated by a custom-made MATLAB script and screw axes were defined by manually selecting the screw head and tip. A third line was drawn from the proximal to distal end of the implant. Intersections of the screw axes with the third line were calculated and the screw-to-screw distance was obtained.

Statistical analysis

Statistical evaluations were performed by using SPSS software (SPSS 23; IBM Corporation, Armonk, New York). After verifying normal distribution of the data utilizing Shapiro-Wilk tests, Repeated Measures analysis of variance were employed to detect differences in ΔALDA progression over time between the three groups. Tuckey's B *post hoc* testing was performed for multiple comparisons. For detecting differences in ΔALDA progression with respect to growth, Mann-Whitney U tests were performed due to non-normally distributed data revealed by the Shapiro-Wilk test. P-values were corrected according to Bonferroni for pairwise comparisons. To determine the rate of modulation, the rate of implant extension, the correlation between proximal and total bone growth and the relationship between modulation rate and normalized load, linear regression analyses were performed. For all tests the level of significance was $\alpha = 0.05$.

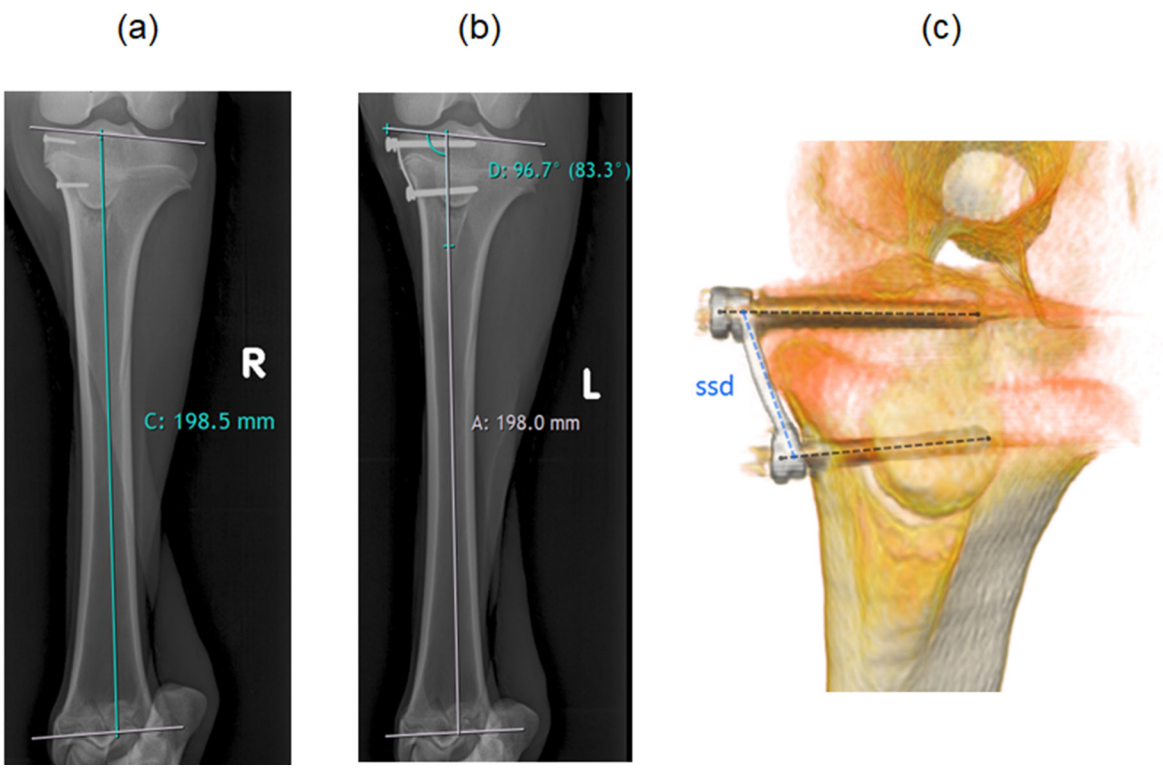

Fig. 3 Measurements of: a) the tibia length (labelled with C), determined by the diaphyseal axis, proximal and distal articular line; b) the tibia length (A) and the articular line-diaphysis angle (D); and c) the implant lengthening by evaluating screw-to-screw distance (ssd) on generated 3D model from CT scans.

Results

No major complications occurred during surgery. In one surgery, one guide wire broke during insertion so that a part remained in the bone. All sheep tolerated the implants well and were able to weight-bear from postoperative day one. Two animals showed a mild fibularis paresis which resolved within a few days. The animals did not reveal problems related to the implant during recovery and throughout the study. Four animals had to be euthanized prematurely due to: 1) acute central nervous symptoms (cerebrocortical necrosis confirmed post-mortem); 2) per acute, reduced general condition and severe anaemia due to Haemonchus contortus (post-mortem diagnosis); 3) fracture of the left metatarsus; and 4) chronic weight loss due to reticuloperitonitis traumatica because of a foreign body (post-mortem diagnosis). Since these events were not directly related to the implant, the obtained data were included until the time of euthanization.

Ovine tibial growth and growth distribution

At surgery the animals were between six and nine months old and had a mean tibia length of 186 mm (SD 10; 167 to 201). During the nine-month treatment period the tibias grew 24.9 mm in mean (SD 4.5; 17 to 31.7). The mean growth was linear, with a mean growth rate of approximately 2.8 mm per month (SD 0.7; 1.1 to 3.4). Linear regression analysis on tibial growth resulted in a factor 0.47 between entire and proximal tibial growth ($R^2 = 0.95$) and revealed roughly equally distributed growth between distal and proximal physis.

Effect of constant force on varus deformity creation

The effect of the different force levels on the developed varus deformity over time is shown in Fig. 4. The highest resulting deformity was achieved in the 200 N group followed by the 120 N group. Marginal effect was observed by using the 60 N implant. Mean ΔALDA at main study completion was 10.6° (SD 3.4) for 200 N, 4.8° (SD 1.8) for 120 N and 0.4°(SD 1.2) for 60 N. These differences were statistically significant between the groups as indicated by individual statistical subsets (Tuckey's B). Radiographs of exemplary cases from each group are given in Fig. 5.

Since the created deformity depends on the occurred growth, a second analysis showing the ALDA change in relation to the growth was performed (Fig. 6).

In agreement with the time-based analysis, the implant with the highest force (200 N) was the most effective, whereas the 60 N implant had no effect. A medium effect was observed in the 120 N group. Statistically significant differences ($p < 0.001$) between all groups were observed. Resulting from the slope of the linear regression the modulation rates were 0.51°/mm for 200 N group,0.23°/mm for 120 N group and 0.05°/mm for 60 N group. Since the proximal tibial growth was approximately 50% of the total bone growth the corresponding modulation rates for the proximal tibia were 1.02°/mm (200 N), 0.46°/mm (120 N) and 0.1°/mm (60 N).

In addition, as indicated in Fig. 7, the mean modulation rates of the 120 N and 200 N implants remained constant over the treatment period. The linear regression analysis in Fig. 8 revealed a distinct linear correlation between the

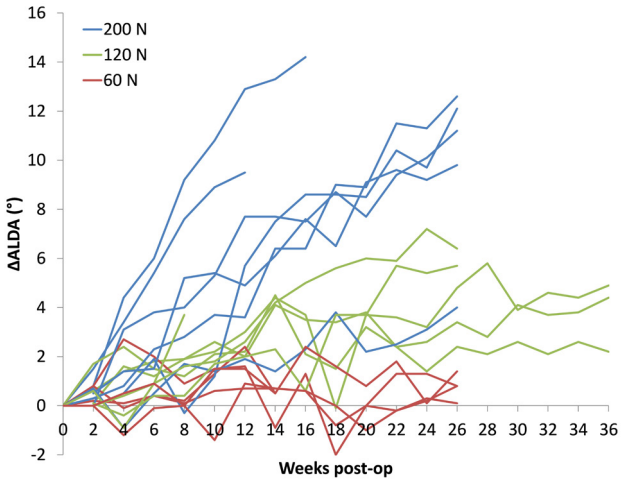

Fig. 4 Articular line-diaphysis angle progression (ΔALDA) over time. Each curve represents one animal (blue = 200 N, green = 120 N and red = 60 N).

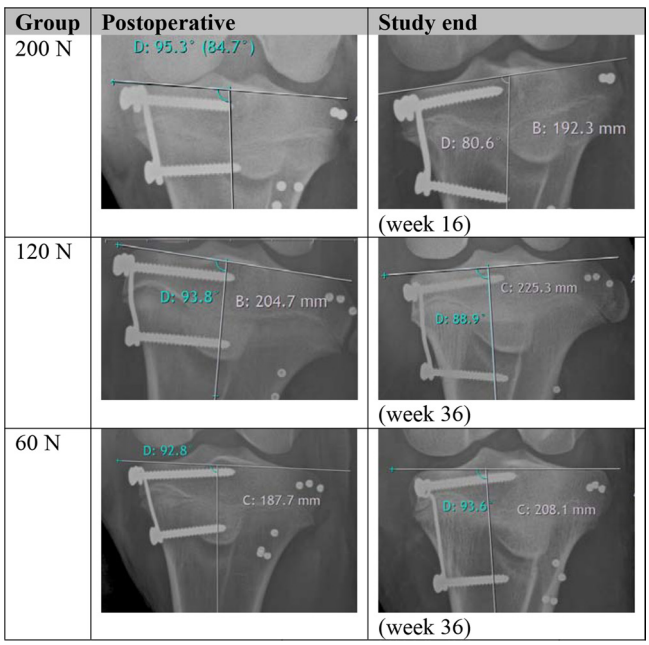

Fig. 5 Radiographic posteroanterior images from postoperative stage and study end, showing the resulting varus deformities for the corresponding force groups

JOURNAL OF CHILDREN'S ORTHOPAEDICS

applied normalized loads and the resulting modulation rates ($R^2 = 0.91$).

Implant function

During the study no implant-related adverse events were observed. In one of the operated animals the distal screw showed a tendency to loosen, therefore, slightly longer screws were used subsequently. Screw loosening was no longer observed. The implant unwinding mechanism was confirmed by measuring the implant elongation. A linear relationship between implant extension and growth was revealed from regression analysis shown in Fig. 9. The implant with the lowest force (60 N) showed fastest extension with a rate of 0.37 mm per 1 mm of growth. A lower extension rate (0.23 mm/mm) was observed in the 120 N group and lowest extension was measured in the 200 N group with a rate of 0.08 mm/mm. This shows that unwinding worked for all groups. All 60 N implants reached the predefined breaking point between week 24 and 28 and detached as planned after 6 mm extension. A detached wire situation of a 60 N implant can be seen in Fig.10. At implant removal/euthanasia, soft-tissue encapsulation was noted in individual animals, bone tissue formation around the implant was not observed. An effect of tissue ingrowth on the unwinding mechanism could not be detected since linear and sustained elongation happened in all groups (Fig. 9).

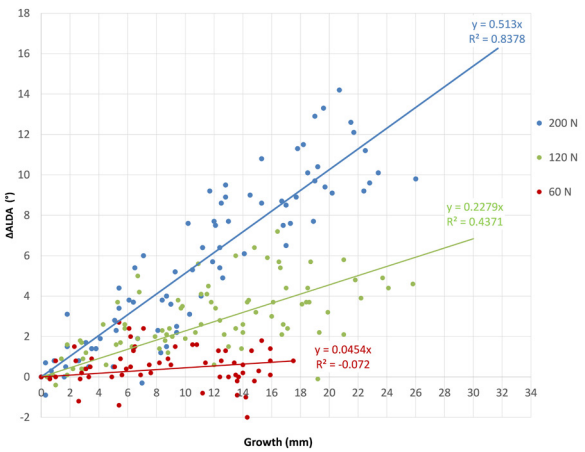

Fig. 6 Functional relationship between magnitude of deformity per millimetre growth. Each dot represents the created deformity to the corresponding growth and the regression lines provides the modulation rates of each group (ΔALDA, change of articular line-diaphysis angle).

Rebound observation

Five animals of the 200 N group and two of the 120 N group had created a significant deformity at the end of the active phase and were consequently included in the rebound observation phase. In an additional surgery the implants were removed and ΔALDA and growth was further assessed. Changes of ALDA between the main study

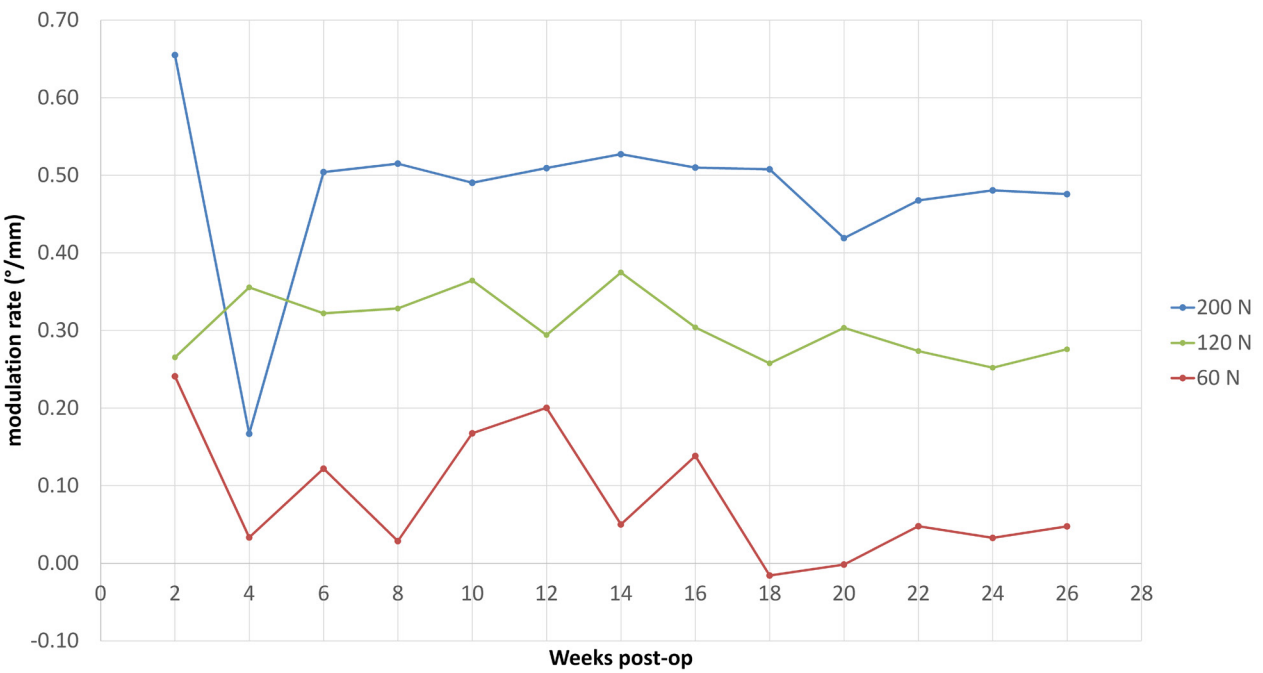

Fig. 7 Mean modulation rate over treatment period. Valley at four weeks in the 200 N group is caused by an outlier in the measurement.

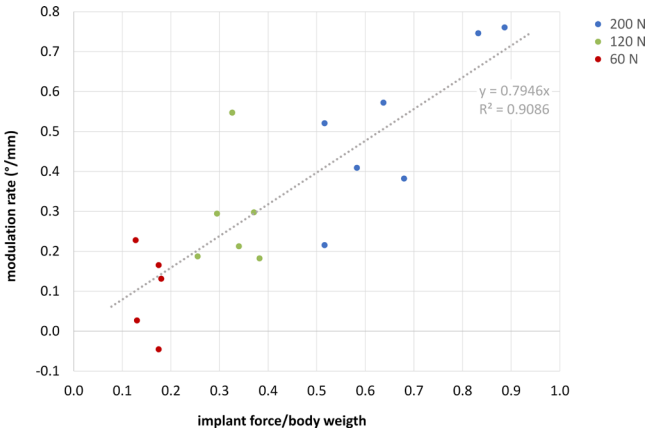

Fig. 8 Linear relationship between modulation rate and normalized loading ratio. Dots are the individual modulation rates related to the implant force to body weight ratio.

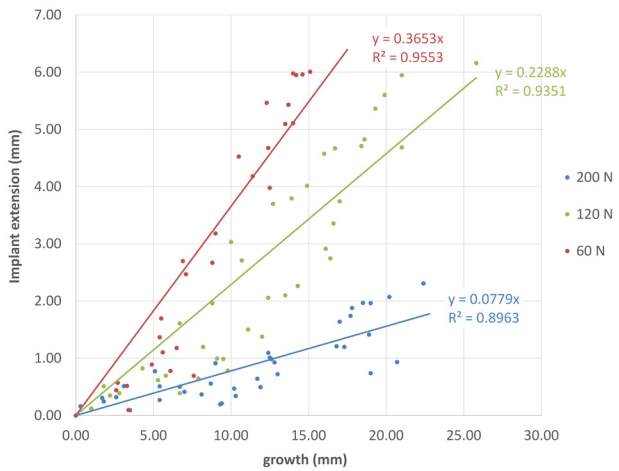

Fig. 9 Implant extension with respect to the growth. Data points represent the implant lengthening at the corresponding growth for all animals of a group. Linear regression lines provide the extension rates of each group.

and rebound phase were compared (Fig. 11). A loss of created deformity was observed in all animals independent of the load level of the implant. Within ten weeks the deformity decreased in mean by 5.2° (SD 1.2) in the 200 N group and by 2.9° (SD 0.1) in the 120 N group. Continued growth was observed in all animals and resulted in a mean total bone growth of 6.9 mm (SD 2.1) within ten weeks, indicating that the growth plates are still open and skeletal maturity has not yet been reached.

Discussion

This large animal experiment showed a safe growth modulation using a novel constant force implant. No commonly reported implant-related failures like excessive screw deformation, implant breakage or extrusion were

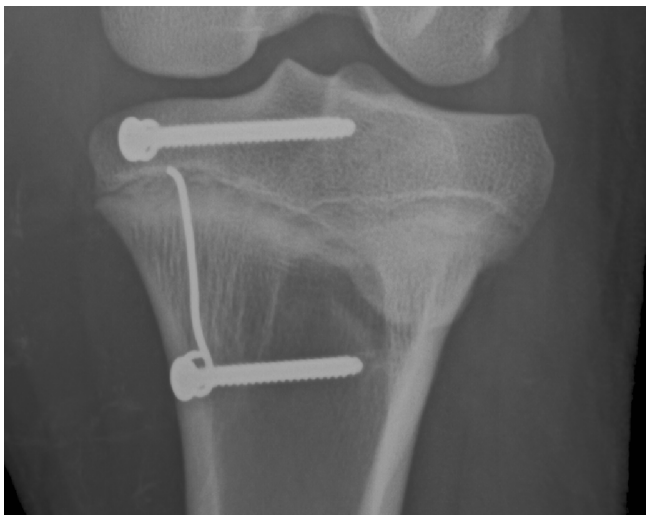

Fig. 10 Radiographic image of an unwound and detached implant.

observed during the study. This is explained by the fact that the load acting on implant and screw cannot exceed the pre-set force limit. Once this level is reached, the wire unwinds instead of rigidly blocking the growth. If the extension range is reached, the wire gently detaches in a controlled manner due to a predetermined breaking point. Feasibility of the unwinding mechanism was confirmed for all force levels by radiographically measured elongation. The predefined breaking mechanism functioned reliably for those implants exceeding the extension range limit of 6 mm. These features render the implant concept passively safe by prevention of excessive force generation at implant and physis. In contrast, with commonly used fixations the reaction force is not controllable and increases steadily with growth.[8] Adverse events such as implant deformation, extrusion or breakage are frequently observed when using Blount staples.[2,3] Use of multiple staples might prevent these incidents but could lead to higher forces acting on the physis and consequently to permanent physeal closure.[9] Although these risks are mainly associated with physeal stapling, they may also occur with TBP. Once the screws of the TBP fixation reach maximum divergence they behave similarly to staples.[10,11] Schroerlucke et al[22] reported screw breakage in 26% of their cases treated with TBP. Although this mainly occurs in children suffering from Blount's disease, it implies a considerable risk for mechanical failure. The new implant concept can be advantageous for these cases due to its safety aspects.

The evaluation showed that reliable growth modulation was possible by using the constant force implant. Depending on the force level applied, low (60 N), medium (120 N) and high (200 N) three statistically different magnitudes of ALDA deformity were created. The highest deformity was

JOURNAL OF CHILDREN'S ORTHOPAEDICS

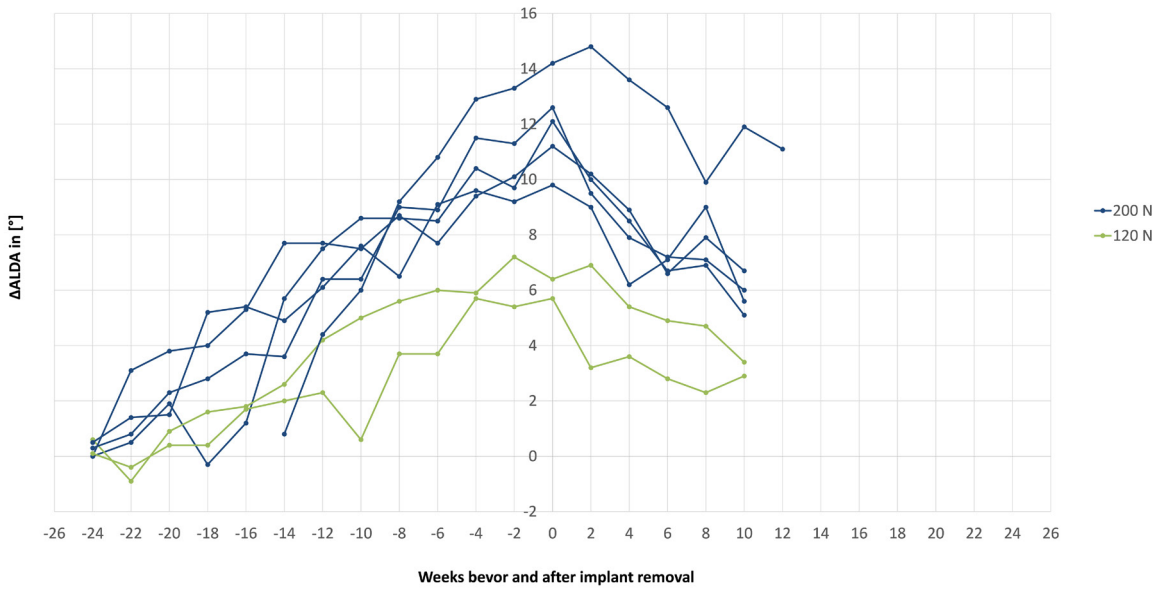

Fig. 11 Changes of articular line-diaphysis angle (ΔALDA) during main study and rebound investigation. Time axis zero was shifted to the time point of implant removal.

achieved with the 200 N implant followed by the 120 N implant. Marginal effect was observed in the 60 N group. The 120 N implant acted slower and less aggressively than the 200 N implant, which could be more physiological for the physis. Histological investigation on mini pigs by Ding et al[23] showed that higher loads lead to greater response of the growth plate after implant removal. The reaction was a faster resumption of growth, which led to recurrence of the deformity. This rebound effect is a common issue in temporary hemi-epiphysiodesis.[7,21,24] A similar tendency was observed in our rebound investigation. Although the relative loss of deformity was of similar magnitude in both groups (44%, 200 N and 47%, 120 N) the rate of rebound was 2.9° within ten weeks in the 120 N group less pronounced than in the 200 N group (5.2° within ten weeks). Moreover, it appears that there is a dependency between rebound rate and rate of deformity creation. Both were similar: 4.8° creation rate and 5.2° rebound rate in the 200 N group; and 2.3° creation rate and 2.9° rebound rate in the 120 N group. The faster the deformity was developed, the greater the rebound rate was. By applying a lower force level, a prolonged treatment period is expected due to the lower modulation rate, but this could be balanced by slower appearance and less pronounced rebound. It is noted that these results should be interpreted carefully because of the small sample size (only two animals in the 120 N group) and the model used (creating deformities instead of correcting) which may influence the results. Further investigations are necessary for a conclusive statement. Nevertheless, the rebound investigation showed that neither 120 N nor 200 N caused physeal closure as growth resumed after implant removal.

A comparison of these findings to other pre-clinical studies is difficult because of different models used. Bonnel et al[18] and Stokes et al[19,20] proved in their *in vivo* experiments the principle of inhibiting bone growth by constant load. Both groups used an external research apparatus for applying constant force to the entire physis aiming at reducing the longitudinal bone growth. They showed that the achieved correction depended on the magnitude of applied load, which is in line with our findings. However, due to different animal species (rabbit, rat, cow) and loading conditions (load applied to the entire physis), a direct comparison of the results must be handled with caution.

As a further assessment parameter, we introduced the modulation rate as a function of angular change per growth measured at the contralateral limb. This approach differs from the literature where modulation rates (correction rates) are mainly reported as angular change per month.[7,25,26] However, the time-based relationship has the disadvantage that it can lead to inconsistent results if growth rates are different, e.g. due to gender or age. This was also observed in our study. One animal of the 200 N group grew considerably slower than the others and, therefore, developed less deformation. Relating the angular change to growth, these results became consistent to allow a uniform assessment. As a further result, it was shown that the modulation rates of the 120 N and 200

N implant remained constant over the treatment period. This also indicates an immediate postoperative effect of the implant. This is advantageous in comparison with TBP where the correction rate varies over the treatment duration. In pre-clinical experiments, Sanpera et al[11] and Goyeneche et al[17] found slower rates at early correction for TBP compared with staples, which is explained by an immediate exertion of compression with staples, whereas TBP will likely become effective only after compression has built up. This is supported by results from a finite element simulation study,[27] which showed that, starting from a lower initial force, the reaction forces increase exponentially during TBP. In contrast to a varying correction rate, a constant rate is beneficial to allow more predictable treatment planning.

Another interesting observation was the resulting linear relationship between the modulation rate and the applied load when converted to a ratio of implant force to body weight. This factor was introduced to determine the individual loading conditions and to put the magnitude of applied load into perspective. It was found that the slightly higher modulation rates in two animals from the 200 N group were due to their lower body weight and the resulting higher loading ratio. This in turn indicates that the physis of the heavier sheep appears to tolerate the force applied by the implant better and produce less deformity than the lighter sheep treated with the same force. This observation should be taken into account when transferring the applied forces to the human application.

To put the results into a clinical context, the obtained modulation rates can be compared with the correction rates of clinical TBP. The mean rates at the human tibia are reported as 0.58°/month by Burghardt and Herzenberg,[7] 0.5°/month by Ballal et al[25] and 0.79°/month by Danino et al.[26] The average age during treatment was 9.59,[7] 11.6[25] and 11.35 years,[26] respectively. Based on modulation rates of 1.02 °/mm (200 N implant), 0.46°/mm (120 N implant) and assuming a growth of 6 mm growth/year (0.5 mm/month) at the human proximal tibia,[26,28] the resulting monthly modulation rates of the proposed concept are 0.23°/month for the 120 N implant and 0.51°/month for the 200 N implant. For the average treatment duration of 14.2 months[7] this would result in 3.3° angular change with the 120 N implant and 7.2° with the 200 N implant. The 200 N implant would, therefore, lead to a similar result as in TBP (7.78°).[7] However, these results must be interpreted cautiously. For direct comparison with TBP, a comparative study with control group must follow in the future. The capability of obtaining different correction rates could also offer new options in the treatment planning. In patients who are closer to skeletal maturity and, therefore, have less residual growth, the maximum force implant could be used to achieve the fastest possible correction. Younger patients with higher growth potential, on the other hand, could receive an implant with lower force level to enable less aggressive and more gentle treatment. The study investigated distinct force levels and their effect on growth modulation but did not deliver exact force boundaries for the lower force limit inducing angular deformity and the upper force limit stalling growth. These relevant parameters must be subject to future investigation in a different experimental setup.

The present study has some limitations. Results are specific to proximal ovine tibia and require careful interpretation before translation to human application. The ovine tibial model was selected as it offers anatomical proportions similar to humans. However, due to differences in growth plate sizes, the force levels used are probably not directly transferable to human application. Clinical studies will need to examine whether the results seen in the animal model can be reproduced in patients. As a further limitation, in our model non-pathological growth plates were treated to create a deformity instead of correcting it. Whether the implant concept performs similar in a human pathological setting needs clinical proof.

The proposed implant concept offers a safe, simple, easy to manufacture and cost-efficient solution for the correction of deformities and has the potential to be translated to clinical application. Due to its safety aspects, further applications such as the correction of leg-length discrepancies are conceivable. However, a few aspects must be critically considered before clinical use. The prominent twisted coil and floating wire after detachment might raise concerns regarding potential soft-tissue irritation. All 18 sheep tolerated the implant well and showed no signs of symptomatic hardware or inflammation. The unwinding of the twisted wire from the screw could raise concerns about generation of wear debris. Since the process is very slow, it is questionable whether there is an increased risk compared with other implants. For a final statement regarding the potential risks, however, further investigations are needed.

Conclusion

This animal study showed that by applying a constant compression force to the physis by means of a novel constant force implant concept, an effective regulation of bone growth and thus the correction of VVD is possible. The modulation rate can be effectively controlled by the force level of the implant. Constant modulation rates were observed throughout the treatment, which is believed to be advantageous compared with commonly used fixation. With the proposed constant force concept, safe treatment without implant-related failure was feasible in the frame of our study. However, to transfer this principle to

human application, clinical trials are necessary to confirm whether the results are translatable to the human pathological situation.

Received 16 October 2020; accepted after revision 3 March 2021

COMPLIANCE WITH ETHICAL STANDARDS

FUNDING STATEMENT

This study was performed with the assistance of the AO Foundation via the AOTRAUMA Network (Grant No.: AR2017_04).

ETHICAL STATEMENT

Ethical approval: All applicable international, national and/or institutional guidelines for the care and use of animals were followed. All procedures were approved by the ethical commission of the canton Grisons, Switzerland (Permission 25_2016) and performed in accordance with the Swiss Animal Protection Law in an AAALAC International-accredited facility.
Informed consent: Not required

ICMJE CONFLICT OF INTEREST STATEMENT

MW reports patent WO2018064781A1 pending, outside the submitted work.
MS reports patent WO2018064781A1 pending, outside the submitted work.
The other authors declare no conflict of interest relevant to this work.

ACKNOWLEDGEMENTS

We thank Alexander Schiedeck for his contribution on implant development and proof of principle.

AUTHOR CONTRIBUTIONS

JB: Wrote the manuscript, Acquired the data, Contributed to study design, Read and approved the submitted version.
LF: Provided critical revision, Contributed to study design, Read and approved the submitted version.
TFS: Provided critical revision, Interpreted the data, Contributed to study design, Read and approved the submitted version.
SZ: Provided critical revision, Contributed to study design, Read and approved the submitted version.
MS: Developed the idea of the implant concept, Provided critical revision, Contributed to study design, Read and approved the submitted version.
MW: Developed the idea of the implant concept, Provided critical revision, Interpreted the data, Contributed to study design, Read and approved the submitted version.

SUPPLEMENTAL MATERIAL

Supplemental material is available for this paper at https://online.boneandjoint.org.uk/doi/suppl/10.1302/1863-2548.15.200218

REFERENCES

1. **White GR, Mencio GA.** Genu valgum in children: diagnostic and therapeutic alternatives. *J Am Acad Orthop Surg* 1995;3:275-283.

2. **Ghanem I, Karam JA, Widmann RF.** Surgical epiphysiodesis indications and techniques: update. *Curr Opin Pediatr* 2011;23:53-59.

3. **Stevens PM.** Guided growth: 1933 to the present. *Strateg Trauma Limb Reconstr* 2006;1:29-35.

4. **Blount WP, Clarke GR.** Control of bone growth by epiphyseal stapling; a preliminary report. *J Bone Joint Surg [Am]* 1949;31-A:464-478.

5. **Stevens PM.** Guided growth for deformity correction. *Oper Tech Orthop* 2011;21:197-202.

6. **Stevens PM.** Guided growth for angular correction: a preliminary series using a tension band plate. *J Pediatr Orthop* 2007;27:253-259.

7. **Burghardt RD, Herzenberg JE.** Temporary hemiepiphysiodesis with the eight-Plate for angular deformities: mid-term results. *J Orthop Sci* 2010;15:699-704.

8. **Bylski-Austrow DI, Wall EJ, Rupert MP, Roy DR, Crawford AH.** Growth plate forces in the adolescent human knee: a radiographic and mechanical study of epiphyseal staples. *J Pediatr Orthop* 2001;21:817-823.

9. **Aykut US, Yazici M, Kandemir U, et al.** The effect of temporary hemiepiphyseal stapling on the growth plate: a radiologic and immunohistochemical study in rabbits. *J Pediatr Orthop* 2005;25:336-341.

10. **Burghardt RD, Kanellopoulos AD, Herzenberg JE.** Hemiepiphyseal arrest in a porcine model. *J Pediatr Orthop* 2011;31:e25-e29.

11. **Sanpera I Jr, Raluy-Collado D, Frontera-Juan G, et al.** Histological differences between various methods of hemiepiphysiodesis: is guided growth really different? *J Pediatr Orthop B* 2015;24:308-314.

12. **Villemure I, Stokes IA.** Growth plate mechanics and mechanobiology. A survey of present understanding. *J Biomech* 2009;42:1793-1803.

13. **Gottliebsen M, Rahbek O, Hvid I, et al.** Hemiepiphysiodesis: similar treatment time for tension-band plating and for stapling: a randomized clinical trial on guided growth for idiopathic genu valgum. *Acta Orthop* 2013;84:202-206.

14. **Jelinek EM, Bittersohl B, Martiny F, et al.** The 8-plate versus physeal stapling for temporary hemiepiphyseodesis correcting genu valgum and genu varum: a retrospective analysis of thirty five patients. *Int Orthop* 2012;36:599-605.

15. **Kumar A, Gaba S, Sud A, et al.** Comparative study between staples and eight plate in the management of coronal plane deformities of the knee in skeletally immature children. *J Child Orthop* 2016;10:429-437.

16. **Wiemann JM IV, Tryon C, Szalay EA.** Physeal stapling versus 8-plate hemiepiphysiodesis for guided correction of angular deformity about the knee. *J Pediatr Orthop* 2009;29:481-485.

17. **Goyeneche RA, Primomo CE, Lambert N, Miscione H.** Correction of bone angular deformities: experimental analysis of staples versus 8-plate. *J Pediatr Orthop* 2009;29:736-740.

18. **Bonnel F, Peruchon E, Baldet P, Dimeglio A, Rabischong P.** Effects of compression on growth plates in the rabbit. *Acta Orthop Scand* 1983;54:730-733.

19. **Stokes IA, Aronsson DD, Dimock AN, Cortright V, Beck S.** Endochondral growth in growth plates of three species at two anatomical locations modulated by mechanical compression and tension. *J Orthop Res* 2006;24:1327-1334.

20. **Stokes IA, Clark KC, Farnum CE, Aronsson DD.** Alterations in the growth plate associated with growth modulation by sustained compression or distraction. *Bone* 2007;41:197-205.

21. **Corominas-Frances L, Sanpera I, Saus-Sarrias C, et al.** Rebound growth after hemiepiphysiodesis: an animal-based experimental study of incidence and chronology. *Bone Joint J* 2015;97-B:862-868.

22. **Schroerlucke S, Bertrand S, Clapp J, Bundy J, Gregg FO.** Failure of Orthofix eight-Plate for the treatment of Blount disease. *J Pediatr Orthop* 2009;29:57-60.

23. **Ding J, He J, Zhang ZQ, Wu ZK, Jin FC.** Effect of hemiepiphysiodesis on the growth plate: the histopathological changes and mechanism exploration of recurrence in mini pig model. *BioMed Res Int* 2018;2018:6348171.

24. **Park SS, Kang S, Kim JY.** Prediction of rebound phenomenon after removal of hemiepiphyseal staples in patients with idiopathic genu valgum deformity. *Bone Joint J* 2016;98-B:1270-1275.

25. **Ballal MS, Bruce CE, Nayagam S.** Correcting genu varum and genu valgum in children by guided growth: temporary hemiepiphysiodesis using tension band plates. *J Bone Joint Surg [Br]* 2010;92-B:273-276.

26. **Danino B, Rödl R, Herzenberg JE, et al.** Guided growth: preliminary results of a multinational study of 967 physes in 537 patients. *J Child Orthop* 2018;12:91-96.

27. **Schneider M, Buschbaum J, Joeris A, et al.** Biomechanical investigation of two long bone growth modulation techniques by finite element simulations. *J Orthop Res* 2018;36:1398-1405.

28. **Whitaker AT, Vuillermin C.** Lower extremity growth and deformity. *Curr Rev Musculoskelet Med* 2016;9:454-461.